Journal of Structural Biology 170 (2010) 32–40

Contents lists available at ScienceDirect

Journal of Structural Biology

journal homepage: www.elsevier.com/locate/yjsbi

Structural characterization of the organic solvent-stable cholesterol oxidase from *Chromobacterium* sp. DS-1

Martin Sagermann [a,b,*], Akashi Ohtaki [a,c], Keith Newton [a], Noriyuki Doukyu [d]

[a] Department of Chemistry and Biochemistry, University of California, Santa Barbara, CA 93106-9510, USA
[b] Interdepartmental Program in BioMolecular Science and Engineering, University of California, Santa Barbara, CA 93106-9510, USA
[c] Department of Biotechnology and Life Science, Tokyo University of Agriculture and Technology, 2-24-16 Naka-cho, Koganei, Tokyo 184-8588, Japan
[d] Bio-Nano Electronic Research Center, Toyo University, 2100, Kujirai, Kawagoe Saitama 350-8585, Japan

ARTICLE INFO

Article history:
Received 11 September 2009
Received in revised form 19 January 2010
Accepted 21 January 2010
Available online 25 January 2010

Keywords:
Cholesterol
Oxidase
Organic solvent-stability
Oxygen channel

ABSTRACT

Cholesterol oxidase is of significant commercial interest as it is widely used as a biosensor for the detection of cholesterol in clinical samples, blood serum and food. Increased stability of this enzyme with regards to temperature and different solvent conditions are of great importance to the reliability and versatility of its applications. We here report the crystal structure of the cholesterol oxidase of *Chromobacterium* sp. DS-1 (CHOLOX). In contrast to other previously characterized cholesterol oxidases, this enzyme retains high activity in organic solvents and detergents at temperatures above 85 °C despite its mesophilic origin. With the availability of one other homologous oxidase of known three-dimensional structure, a detailed comparison of its sequence and structure was performed to elucidate the mechanisms of stabilization. In contrast to factors that typically contribute to the stability of thermophilic proteins, the structure of CHOLOX exhibits a larger overall cavity volume, less charged residues and less salt bridge interactions. Moreover, the vast majority of residue substitutions were found on or near the protein's solvent exposed surface. We propose that the engineering of enhanced stability may also be accomplished through selective engineering of the protein periphery rather than by redesigning its entire core.

1. Introduction

Human arteriosclerosis, hyperlipemia as well as obesity are diseases that have been associated with an imbalance of cholesterol. Accurate determinations of this lipid is thus of fundamental importance to the diagnosis and prevention of diseases that result from unhealthy concentrations of this compound. Today, the majority of cholesterol quantitations are performed by a protein-based biosensor consisting of multiple enzymes including cholesterol oxidase. With the exception of glucose oxidase, this enzyme has become one of the most widely used biosensors in clinical applications (MacLachlan et al., 2000). This enzyme, which is derived from a prokaryotic organism, is uniquely capable of translating the amount of sample cholesterol into a readable signal, H_2O_2, for many optical or electronic devices (MacLachlan et al., 2000).

In order to enhance the accuracy of the measurements, prior isolations of the lipid are frequently required. For this purpose, organic solvents are used for the solubilization and extraction of lipidic compounds from biological membranes. Moreover, organic solvents are also utilized frequently to facilitate chemical modifications and for the immobilization of sensor proteins onto polymer matrices and electrodes (Arya et al., 2009; MacLachlan et al., 2000; Wu and Choi, 2003). Unfortunately, however, many of these commonly used solvents denature proteins, limiting their applicability dramatically (Doukyu and Aono, 2001). Strong interactions of the solvents with the protein and the withdrawal of water molecules from the protein can often lead to disintegration of structure and function.

Based on their wide ranging and unique thermal stabilities, the search for suitable enzymes has mainly focused on thermophilic organisms as their stabilities appear attractive for many medical and industrial applications (Egorova and Antranikian, 2005).

Recently, we have identified a new cholesterol oxidase from *Chromobacterium* sp. DS-1 (CHOLOX) (Doukyu and Aono, 2001). This enzyme belongs to the type II cholesterol oxidases, which have the FAD cofactor covalently attached to the protein. In contrast to oxidases from other organisms, this enzyme still functions in most organic solvents and detergents, as well as at high temperatures. While most of the commercially available enzymes loose their activity upon a 30 min incubation at 50–75 °C, remarkably, this enzyme retained 80% of its activity after incubation at 85 °C, i.e. hyperthermal conditions, rendering this enzyme as the most stable to date (Doukyu et al., 2008, 2009). Until now, only one other homologous structure of this enzyme class from *Brevibacteri-*

* Corresponding author. Address: Department of Chemistry and Biochemistry, University of California, Santa Barbara, CA 93106-9510, USA. Fax: +1 805 893 4120.
E-mail address: Sagermann@chem.ucsb.edu (M. Sagermann).

1047-8477/$ - see front matter © 2010 Elsevier Inc. All rights reserved.
doi:10.1016/j.jsb.2010.01.012

um sterolicum has been determined (PDBid:1I19, (Coulombe et al., 2001), (here also referred to as BCO)). In contrast to CHOLOX, this enzyme, which is also derived from a mesophilic prokaryote, is only moderately stable to about 50 °C as judged by loss-of-activity measurements at different temperatures (data on systematic melting studies with respect to the enzyme's structure were not available). Furthermore, it is also rapidly inactivated by organic solvents such as isopropanol or detergents like Triton X-405, for example (Doukyu, 2009).

In order to understand the differences of its physical properties in comparison to its mesophilic counterpart BCO, we have determined the crystal structure to 1.54 Å resolution. In this study, we take inventory of the respective amino acid compositions, cavity volumes, number of interactions and distributions of electrostatic potentials and compare it to other thermophilic/solvent stable enzymes. Furthermore, we characterize the structural distribution of residues that are unique (non-conserved) to CHOLOX but not to BCO as they are most likely to contribute to the superior stability of the enzyme. These residues will be referred to as "new" residues in the text.

2. Materials and methods

2.1. Purification

Purification of the enzyme was performed as previously reported (Doukyu and Aono, 1998). Briefly, a 25 mL overnight culture of CHOLOX–plasmid bearing BL21 *Escherichia coli* cells were grown in 1 L shaker flasks in the presence of 1 μM ampicillin. 1 μM IPTG was added at an OD_{600} of 0.6. Subsequently, induction was carried out for 3 h before harvest with a centrifuge (Beckmann Rotor JA10, 4000 rpm for 30 min). The resultant cell pellet was either stored at −75 °C or lysed directly using the French-Press operated at 1200 PSI. The cell homogenate was submitted to a high-speed centrifugation spin (Beckman Rotor JA20, at 12,000 rpm). The supernatant was collected (typically approximately 50 mL) and incubated immediately in a water bath at 80 °C for approximately 45 min to denature soluble *E. coli* proteins. The homogenate was then submitted to another high-speed centrifugation and the resultant supernatant was loaded onto a DEAE–Sepharose column (Merck). The mostly pure enzyme was collected in the flow-through fraction, concentrated and dialyzed against Standard Buffer (50 mM Tris, pH 8.2, 100 mM NaCl and 1 mM EDTA).

2.2. Crystallization

Prior to crystallizations, the protein solution was concentrated to approximately 3 mg/mL. Initial crystallizations were carried out with commercially available screens from Hampton (Crystal Screens I + II) and Jena Bioscience GmbH (JB Screen HTS II). Optimal conditions for crystal growth were identified with 500 mM ammonium sulfate, 1.0 M lithium sulfate and 10 mM sodium citrate. Crystals were readily identified by their yellow color.

2.3. Data collection and processing

Data collections were performed at the Stanford Synchrotron Radiation Laboratory, beamline 7-1. For this purpose, crystals were incubated with the addition of 5% sucrose into the mother liquor for one hour prior to flash-freezing in liquid nitrogen. Data integration, reduction and scaling were carried out with the programs XDS, and XSCALE (Kabsch, 1993). The structure was determined by molecular replacement using the program AMoRe (CCP4, 1994; Trapani and Navaza, 2008) using the structure PDBid:1I19 as a search model. Subsequently the structure was refined using the programs CNS (Brunger et al., 1998) and REFMAC5 (CCP4, 1994; Murshudov et al., 1997). A random-selected invariant number of reflections (4.6%) was maintained as a test set throughout the refinement calculations (Adams et al., 1997). The final statistics on data collection, reduction and refinement are shown in Table 1. Superpositions and structural comparisons were carried out with the program DALI (Holm et al., 2008). Electrostatic surface potentials were calculated with the program APBS (Baker et al., 2001) and rendered and displayed with the program VMD (Humphrey et al., 1996). The number of salt bridges was also determined with this program. Volume and cavity calculations were performed with the program VOIDOO using a 1.4 Å probe radius and default parameters (Doukyu and Aono, 2001; Kleywegt and Jones, 1994). Packing efficiencies as defined by Pattabiraman et al. (1995) and Voss and Gerstein (2005) were calculated using the program OS or the Voronoi Packing Efficiency Calculator.

3. Results

3.1. Overall structure

The structure of CHOLOX (residues 1–540) closely resembled the structure of BCO (residues 57–613) (Coulombe et al., 2001), which is reflected by the pronounced sequence identity of 44.9%. Both peptide backbones superimpose with ca. 1 Å rmsd accuracy (Fig. 1). As it is expected for class II enzymes, the prosthetic group, FAD, was covalently bound to His63 *via* the C8 methyl of the flavin group. The most pronounced structural differences between the two proteins were observed in loop regions. In comparison to BCO, a structural sequence alignment with the program DALI exhibited three small insertions (totaling four residues, i.e. at positions 181–182, 314 and 492), and only one 3-residue deletion,

Table 1
Crystallographic data and refinement statistics.

Data set	CHOLOX
X-ray source	BL7-1
Cell dimensions (Å)	
a	62.22
b	90.38
c	124.19
Resolution (high res. bin)	40–1.54 (1.62–154)
Wavelength (Å)	0.97949
Space group	$P2_12_12_1$
Number of reflections (total/unique)	96,731 (12,447)
Number of reflections (observed)	351,568 (44,270)
R-merge	0.046 (0.347)
$I/\mathrm{Sig}(I)$	21.42 (4.34)
Completeness	93.3 (86.1)
Redundancy	3.63 (3.56)
Refinement	
R_{work}/R_{free}	0.176/0.196
Number of atoms	
Protein	4300
Water	406
Ligands	76
rmsd	
Bond lengths	0.023
Bond angles	2.1

$R_{sym} = \sum|I - \langle I\rangle|/\sum\langle I\rangle$; where I is the observed intensity and $\langle I\rangle$ is the statistically weighted average intensity of multiple symmetry related observation.
R-factors: $R = \sum||F_{calc}| - |F_{obs}||/\sum|F_{obs}|$; where F_{calc} and F_{obs} are the calculated and observed structure factors, respectively. The $R_{(free)}$ was calculated using the same formula with 4.6% of the observed reflections.
rmsd, root-mean-square deviation from ideal geometry.
Coordinates were deposited at the Brookhaven Bank with the Accession No. PDBid = 3JS8.

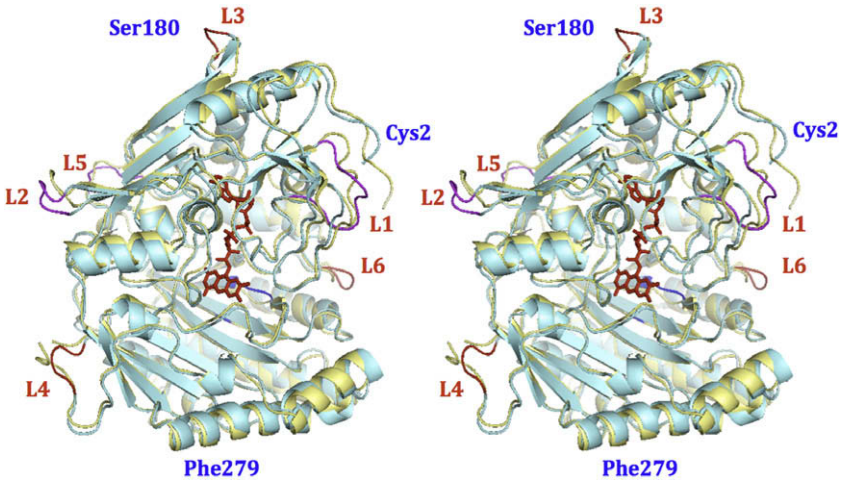

Fig. 1. Stereo diagram of the overall structure of CHOLOX (light blue) superimposed onto the structure of BCO (1I19, yellow). Both structures are shown as a ribbon diagram. The prosthetic group of CHOLOX is presented as a red stick model. Both main chain structures superimpose with an accuracy of about 1 Å rmsd. Conformational variations are mostly observed in loop structures (L1: 70–78, L2: 95–99, L3: 178–182, L4: 273–280, L5: 415–419, L6: 485–488) as well as in an extended strand conformation that faces the substrate-binding site (in purple, behind the FAD). Figs. 1, 2, 4 and 5 were prepared with the program PyMol (http://pymol.sourceforge.net/).

between residues 277 and 279, thus maintaining the relative lengths of the structures. All of the resulting structural changes were located in solvent-exposed loop or turn structures. Large conformational differences were found in loops L1–L6 (Fig. 1). Another significant structural divergence was found in the core of the protein between residues 358 and 361. It is located in proximity to the substrate-binding cavity. In the structure of *BCO*, the sequence 'EGGG' (between residues 432 and 435) is replaced by the sequence 'ANGY' in CHOLOX (residues 358–361) (see structural alignment in Supporting Information), whereby the large tyrosine side chain is likely to require a repositioning of the C_α of Gly360 by more than 4 Å (Fig. 2).

3.2. Protein volume and density

The overall volumes of both proteins (calculated with VOIDOO) were also very similar with 54,330 $Å^3$ for CHOLOX and 55,830 $Å^3$ for BCO. Since CHOLOX and BCO contain about the same number of atoms (CHOLOX:4179, BCO:4368), the overall packing efficiencies as defined by the percentage of well-packed residues (Pattabiraman et al., 1995; Voss and Gerstein, 2005) were also comparable (CHOLOX: 40.4%, BCO: 39.1%), albeit somewhat higher for CHOLOX. (The calculation was performed on the protein- and FAD atoms only and in the absence of waters.) These indiscriminate differences between the packing efficiencies therefore confirm earlier observations of mesophilic and thermophilic proteins (Karshikoff and Ladenstein, 1998). As shown in Table 2, the respective buried surface areas for apolar residues were also similar in both enzymes. However, some differences were observed in buried polar surface areas.

3.3. Substrate cavity

Class II cholesterol oxidases contain a large central cavity that is used to bind the steroid substrate. As the position of the FAD as well as most of the surrounding residues have remained the same, the substrate cavity volume has also remained similar (Fig. 3) (Doukyu and Aono, 2001). Overall cavity volume calculations with the program VOIDOO (Doukyu and Aono, 2001; Kleywegt and Jones, 1994) in the absence of multiple conformers of residues and in the absence (or presence) of the prosthetic groups (FAD) showed dramatic differences between the two structures. Despite

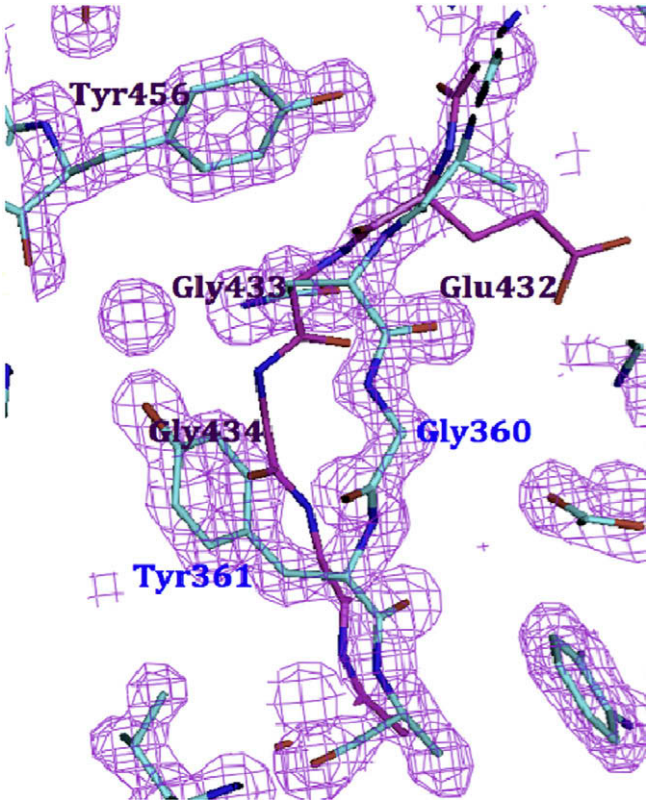

Fig. 2. Structural divergence in the core of the protein. $2F_oF_c$ electron density (at 1.54 Å resolution and contoured at 1.6σ above the mean) surrounding strand 8 between residues 358 and 361of CHOLOX (blue) and the corresponding superimposed strand of BCO (purple). Both strand structures are shown as a stick model. The density as well as simulated-annealing-omit maps (CNS (Brunger et al., 1998), not shown) confirm that the new position of this strand is most likely a consequence of the bulky Gly-to-Tyr residue change. As a result, Gly360 of CHOLOX appeared translated by more than 4 Å in comparison to the corresponding Gly415 residue of BCO. This conformational change is also concomitant with a reduction of available cavity volume in the vicinity of the FAD.

the same 15 cavities in both proteins, a much larger overall cavity volume of 615.4 A^3 in CHOLOX was observed in contrast to the overall cavity volume of 564.2 A^3 of BCO.

Table 2
Surface, volume and packing statistics.

Protein	CHOLOX	BCO
Total occluded surface (Å^2)	31,849	32,987
Occluded apolar surface (Å^2)	18,525	18,392
Occluded polar surface (Å^2)	*13,321*	*14,195*
Total exposed surface area (Å^2)	21,827	22,010
Exposed apolar surface (Å^2)	10,610	10,287
Exposed polar surface (Å^2)	11,218	11,722
CHASA (A^2)	7796.7	8083.02
Protein volume (A^3)	54,330	55,830
Cavity volume (A^3)	*615.4*	*564.2*
Packing density	0.403	0.394
Number of salt bridges with 3.2 Å cut-off	*19*	*23*
Number of salt bridges with 4.0 Å cut-off	*25*	*30*
Number of salt bridges with 7.0 Å cut-off	*54*	*73*

Occluded (buried) and exposed surface areas as well as the packing densities were calculated with the program OS or VORONOI. Protein and cavity volumes were calculated with the program VOIDOO and the number of salt bridges were determined with the program VMD (VOIDOO calculations were performed in the absence of FAD). For the extraction of the specific surface areas, polar and an apolar residues were defined as: asn, asp, arg, cys, gln, glu, his, lys, tyr, ser, thr; or: ala, gly, ile, leu, met, phe, pro, trp, val, respectively. Substantial differences are italicized.

3.4. Structure of the channel

The structure determination of the *Brevibacterium* enzyme identified a small hydrophobic channel that extended from the substrate cavity out to the solvent exposed surface of the protein (Coulombe et al., 2001). Even though not all residues in the corresponding regions in the two proteins are conserved, this channel was also present in CHOLOX albeit with a somewhat altered position and shape (Fig. 3). The inside of the channel is to some extend hydrophobic and filled with eight clearly defined densities that were interpreted as waters.

In contrast to BCO, this channel was connected to yet another shorter channel that further extends its volume to result in a horseshoe shaped appearance. In addition to these structures, other smaller cavities were observed throughout the protein that, on the whole contribute to the 34% larger cavity volume.

Direct access from the substrate cavity into the hydrophobic channel is interrupted only by the presence of the Arg403 side chain (Fig. 4). A similarly positioned arginine residue was also found in the structure of BCO (Arg477) and it has been proposed to function as a solute gate (Coulombe et al., 2001). In the structure of BCO, this residue assumes two different conformations: one that closes the channel and a second in which the side chain is reoriented to form a salt bridge with the nearby Glu475 that opens the channel. In the structure of CHOLOX, only the closed conformation was observed. Even though no clear densities for alternative conformations were evident, the *B*-values for Glu401 and the Arg403 were substantially higher than those for any of the neighboring residues suggesting increased structural flexibility. A recent mutagenic study on the BCO enzyme also implied that the nearby Glu311 may also be of importance to the function of this gate and thus the enzyme's catalytic efficiency (Piubelli et al., 2008). A similarly positioned Glu255 was also found in the structure of CHOLOX. Its density, however, is well defined and its *B*-values are comparably low suggesting low conformational flexibility.

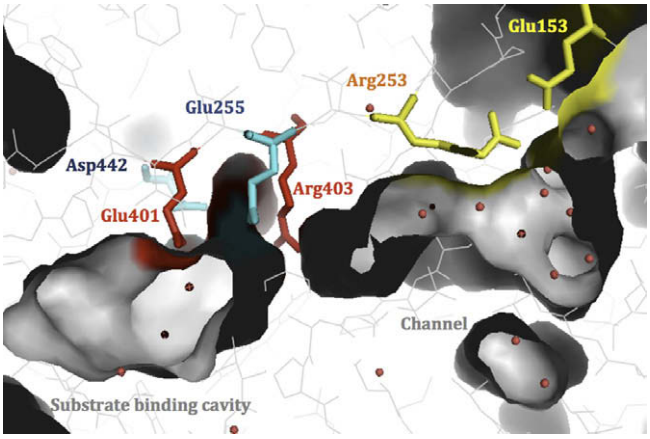

Fig. 4. Close-up view of the channel structure. Shown is the structure of CHOLOX with the channel surface structure displayed in gray. The viewing perspective is similar to that of Fig. 3. The channel extends from the substrate-binding site to the surface of the protein. The refined water molecules are shown as red dots. Amino acids that are proposed to be involved in the gating mechanism are shown in red (Arg403 and Glu401). Glu255 and Asp442 (blue) are in direct vicinity and are likely to influence their electrostatic environment. On the other side of the channel is Arg253-Glu153 salt bridge. Disruption of this interaction could possibly also lead to a channel closure as a result of a reorientation of the arginine residue.

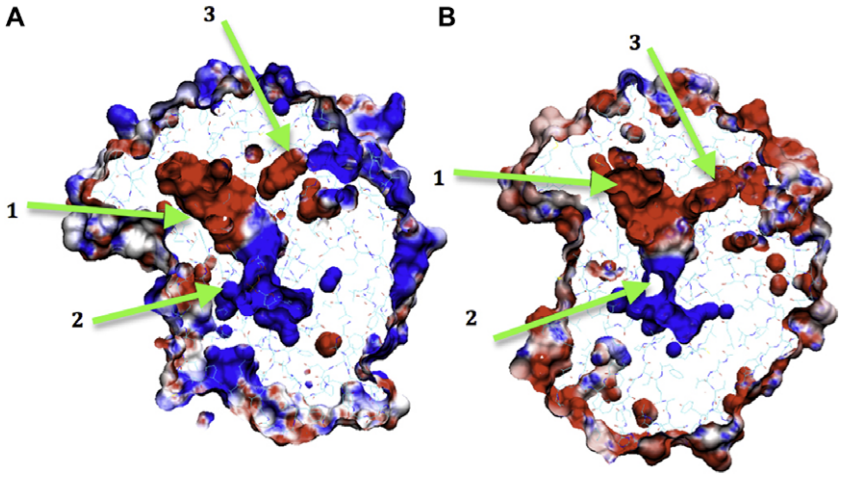

Fig. 3. Solvent accessible surface representation of CHOLOX and BCO. The surface is colored according the electrostatic surface potential as defined and calculated by the program APBS. Positively charged areas are colored in blue and negatively charged areas are shown in red. A slice through the structure of ~10 Å is shown to illustrate the large cavity system. The FAD group is bound with its negatively charged phosphate groups to the blue portion of the cavity (arrow 2) whereas the substrate-binding pocket is located in the red portion (arrow 1). The channel structure that connects the substrate-binding cavity to the surface is highlighted (arrow 3). In the structure of CHOLOX, this connection interrupted due to the "closed" conformation of Arg403.

Another charged residue in the vicinity of the gate was observed that is likely to interact with the gating residues as well. Asparagine Asn516 of BCO was replaced by Asp442 in CHOLOX, whereas Glu432 of BCO was substituted by Ala358 thus resulting in a "repositioning" of the carboxyl group within the vicinity of the gating residues (Fig. 4). Despite this new position of the carboxyl (of Asp442), the conserved Lys480 of CHOLOX is still well positioned to interact with it, as well as with the conserved Glu477 (Glu551 in BCO). Furthermore, Glu477 also maintains an indirect interaction with Arg403 *via* a water molecule. A similar interaction was also found in the BCO enzyme. Consequently, the substrate-binding site and the proposed access gate of the channel of both proteins were surrounded by a network of charged residues, water molecules and salt bridge interactions that appeared to be conserved among the oxidases as judged by sequence alignments as well as structural comparisons.

Interestingly, the other site of the channel that faces the solvent also exhibited a salt bridge between residues Arg253 and Glu153 (Fig. 4). In BCO, the corresponding positions are occupied by Gly309 and Gln211, respectively. Systematic model building suggests that breaking this interaction could also result in a reorientation of the arginine side chain to close the channel. In contrast to the above-mentioned Arg403-Glu401 interaction, however, this salt bridge in CHOLOX appeared strong and stable as judged by the low *B*-values and its well-defined appearance in the omit-electron density. It therefore remains to be shown if these residues are of functional importance.

3.5. Distribution of charged residues

The structure of CHOLOX revealed a surface charge distribution that differed dramatically from that of BCO. As shown in Fig. 5, the electrostatic surface potential showed a somewhat balanced distribution of positive and negative charges. On BCO, on the other hand, a predominantly negatively charged surface was observed consistent with the low isoelectric point of the molecule. Overall, CHOLOX appeared to carry less charged residues than BCO. Even though the number of arginine and lysine residues, was somewhat larger (for arginine: CHOLOX: 27, BCO: 25, for lysine: CHOLOX: 21, BCO: 19), the total number of negatively charged residues was reduced significantly. For example, CHOLOX contains only 26 aspartates and 18 glutamates in contrast to BCO, which contains 27 and 28, respectively (Fig. 6). Accordingly, the number of salt bridges was also less in CHOLOX (Fig. 7). Whereas this protein maintained

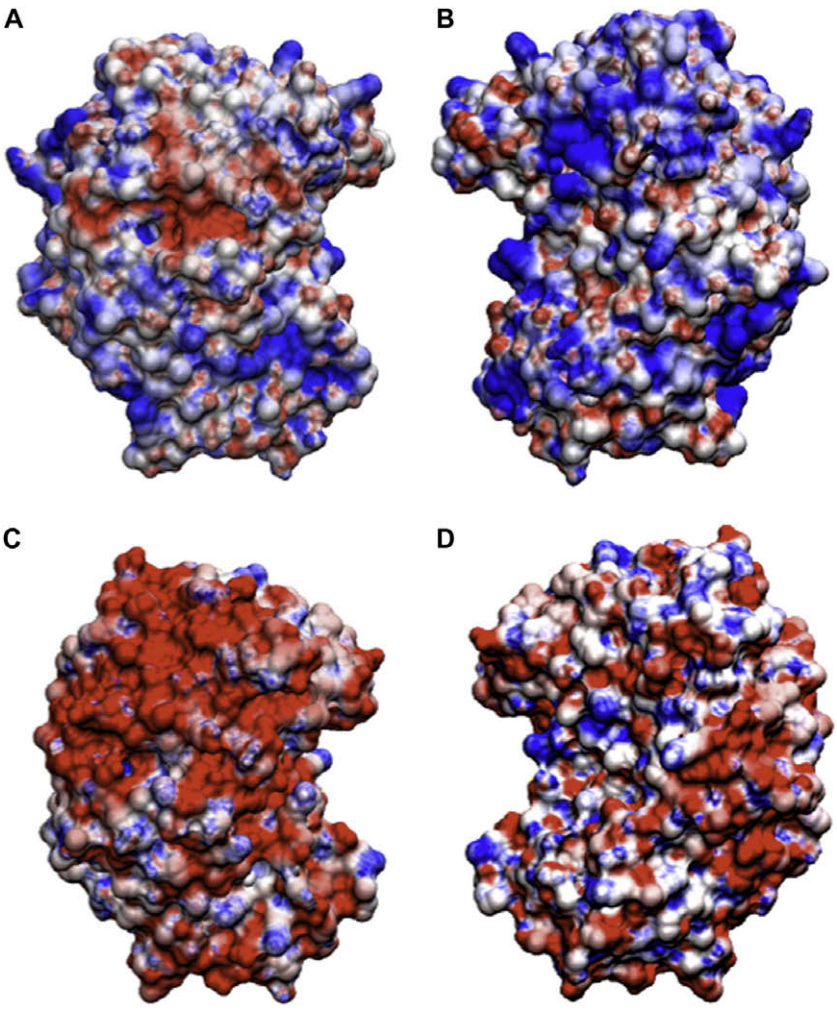

Fig. 5. Electrostatic surface potential of the oxidases. The surface potentials of CHOLOX is shown in front-view (A) and from the back (B). Likewise, the surface potentials for BCO are shown in similar orientation from the front (C) and back (D). A comparison of the two structures reveals that BCO is considerably more negatively charged than CHOLOX. This result is also consistent with the respective isoelectric points of CHOLOX (p*I* = 8.6) and BCO (p*I* = 5.5). Even though BCO has only 11 more negative charges and four more positive charges than CHOLOX, the overall negative charge appearance of the BCO is likely to have resulted from a specific distribution of charged residues rather than a substantial increase in the residue number. Not surprisingly, crystals of both proteins were obtained in the corresponding pH values. This figure was prepared with the programs APBS and VMD.

only 19 salt bridge interactions, a total of 23 interactions were found in BCO (using a 3.2 Å cut-off radius). This relative difference of interactions remains highly similar if larger cut-off values are chosen. This result therefore also appears to contradict previous proteomic studies on thermophilic proteins, that suggest that more ionic charges and interactions may be required to stabilize the proteins efficiently (Perl and Schmid, 2002).

Mapping of all "new" (i.e. non-conserved and unique CHOLOX-) charged residues onto the structure of CHOLOX demonstrated that, with the exception of two residues, Asp442 and His201, all residues were directly positioned at the surface of the molecule (Fig. S7, Supporting Materials). Only the His201 faced a small solvent bearing cavity in the protein's core, whereas the above-mentioned Asp442 was observed near substrate-binding cavity. Of all the "new" charged residues, merely seven were involved in salt bridge interactions.

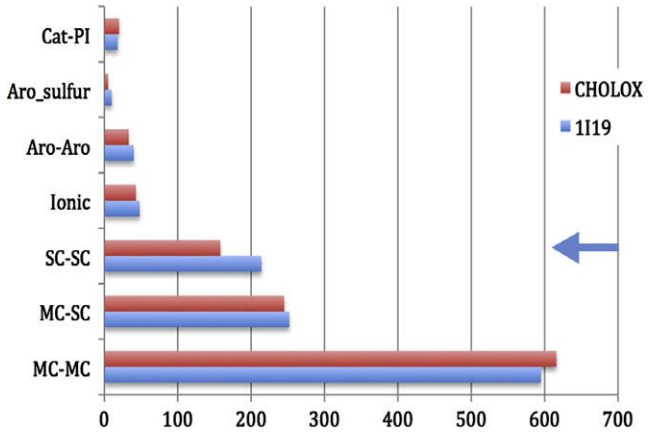

Fig. 7. Frequency of occurrence of selected interactions as determined with the program PIC (Tina et al., 2007). Listed are the interactions main-chain/main-chain (H-bonds) (MC–MC), main-chain/side-chain (H-bonds) (MC–SC), side-chain/side-chain (H-bonds) (SC–SC), interactions between aromatic side chains (Aro-Aro), salt bridge interactions (ionic), aromatic and sulfur side chains (Aro-Sulfur) and cation/pi type interactions (Cat–Pi). Whereas the overall number of specific interactions has remained the same between the two proteins, significantly more side-chain/side-chain interaction were observed in the CHOLOX structure. All interactions were determined within the default cut-off radius of 4.5 Å. The relatively smaller number of salt bridges of CHOLOX also remained if the cut-off radius was changed to 6 Å.

3.6. Serine and threonines

The majority of the serine residues of CHOLOX and BCO are located on the surface of the protein. Consequently, almost all of the "new" serine residues (serine residues that are unique to CHOLOX) are also located on the surface (Fig. S4 (Supporting Materials)). Only two residues were found buried. Previous statistical analysis of serines suggests a low frequency of these residues in thermo-

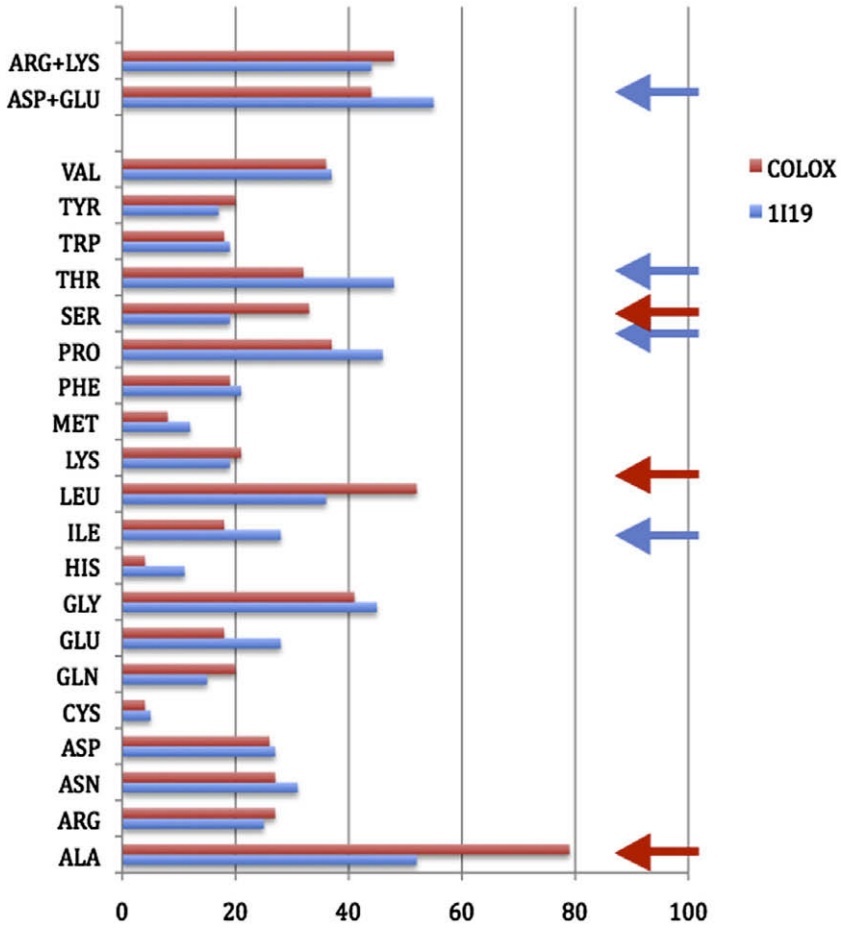

Fig. 6. Amino acid contents of CHOLOX (red) and in 1I19 (i.e. BCO) (blue). Shown are only residues that were resolved in the crystal structures (CHOLOX (540 aa) and 1I19 (541 aa)). Whereas the majority of the respective occurrences have remained similar in both proteins, some substantial differences were observed (highlighted by arrows). CHOLOX appeared to have significantly more alanine and leucine residues but less isoleucine, threonine and prolines. On the contrary, the number of aromatic side chains phenylalanine, tyrosine and tryptophane remained about the same. Among the charged residues, glutamate, aspartate, lysine and arginine, only glutamate was present to a smaller extend in CHOLOX. Prolines, which have been a observed in higher frequencies among thermophilic proteins, appeared to a lesser degree in CHOLOX.

philic proteins (Chakravarty and Varadarajan, 2000; Kumar and Nussinov, 2000). Moreover, Pack et al. found that thermophilic proteins also show lower frequencies of serines in exposed or partially exposed sites (Pack and Yoo, 2004). As the structure of CHOLOX displays considerably more serines than BCO (Fig. 6) and almost all of them were located at solvent accessible locations, the observed high frequency of this residue thus also appeared to contradict earlier statistical findings of thermophilic proteins.

Overall, however, threonine residues appeared less abundant in CHOLOX (Fig. 6). The corresponding positions of the non-homologous residues that are unique to CHOLOX were found in buried as well as surface exposed positions (Fig. S4). The removal of the corresponding polar occluded surface areas (Table 2) may suggest that a withdrawal of hydroxyls may have contributed to a thermal stabilization.

3.7. Glycine, proline, asparagine and glutamine

Prolines and glycines are known to terminate secondary structure elements and are therefore frequently found near turn or loop regions. Consequently they are often highly conserved and are thought to contribute substantially to stability. Accordingly, of the 46 proline residues (and 45 glycine residues), only seven prolines (or 14 glycines) were identified as non-homologous, respectively. All of these residues were found at the solvent accessible surface (with the exception Gly143, 483) (Fig. S6). Asparagines and glutamines (23 residues total) were also found predominantly at solvent exposed sites in this case (exceptions: Asn64, Asn359).

3.8. Hydrophobic residues

Hydrophobic surface area and efficient interdigitation of apolar core residues is thought to contribute majorly to a protein's stability. Recently it was noted that proteins from thermophiles may exhibit a significant increase of buried methyl groups or β-branched residues in conserved hydrophobic core positions (Paiardini et al., 2008). The overall number of isoleucine- and valine-residues of CHOLOX, however, was reduced. Moreover, out of the 36 valines of CHOLOX, only 14 appeared to be strictly conserved. The remaining 22 valine positions were replaced by either alanine, glycine, isoleucine, leucine, threonine, phenylalanine or tryptophane as judged by a CLUSTALW alignment of the two sequences (Fig. S1 in Supporting Information). Similarly, isoleucines were also present to a lesser degree in CHOLOX (Fig. 6). These observations therefore also appeared to contrast previous statistical findings of thermophilic proteins (Kumar et al., 2000; Pack and Yoo, 2004).

Leucine residues, on the other hand, were much more abundant in this protein (CHOLOX: 52, BCO: 36). As expected, the majority of leucines were highly conserved and positioned in the core of the protein. Of all the leucines, the majority of the 28 non-conserved ("new") residues were observed in the periphery of the structure (Fig. S3, Supporting Information). While the side chains themselves were typically buried, most of these residues were positioned on solvent exposed secondary structure elements. In other words, the positions of these "new" leucine residues in the protein's periphery may be another indication for specific stabilizations of surface structures.

One of the most dramatic differences between the sequences of CHOLOX and BCO was the significantly increased number of alanine residues. Instead of only 52 residues in BCO, a total of 79 alanine residues were found in the structure of CHOLOX (Fig. 6 and Fig. S2). Sequence-alignments identified only 26 of these residues as conserved (Figs. S1, S2 (Supporting Information)). Mapping of the remaining 53 non-conserved residues onto the structure of CHOLOX showed that about half of these residues (25 residues total) were located on the solvent exposed sites of α-helices. The remaining alanines were either located in loops, turns (24 residues), or sheets (only four residues). The large number of these "new" alanine residues in helices may be indicative of specific helix-stabilization. Previous studies have revealed that the engineering of alanines into helices can stabilize a protein considerably (Arnott et al., 2000; Blaber et al., 1993, 1994; Lin et al., 1994) *via* its favorable helix-forming propensity. Conversely, the introduction of alanine residues into β-strands was shown to have a destabilizing effect on a protein (He et al., 2004), which may be consistent with the very low number of "new" alanines observed in the strands of CHOLOX.

The vast majority of the alanines were observed at the solvent accessible surface of the protein. Due to the lack of a large side chain, these residues may permit solvent molecules to contact the protein backbone directly. In particular the carbonyl- and amino-groups have been suggested to engage in specific interactions with the solvents (Blaber et al., 1995). Such interaction sites, in particular, have been proposed to occur at polyalanine stretches of helices possibly causing destabilizations or unfolding of the protein (Sundaralingam and Sekharudu, 1989). Experimental observations of such engineered polyalanines in exposed sites of T4 lysozyme, on the other hand, have demonstrated some stabilization of the proteins in most cases (Heinz et al., 1992; Zhang et al., 1991). In other words, despite the fact that three regions can be identified in CHOLOX that produce continuous alanine patches on the surface, this protein maintains superior stability against a variety of different solvents – including detergents and alcohols (Doukyu and Aono, 1998). Obviously, as the increase of alanine residues in CHOLOX is by far the most dramatic difference compared to BCO, its net effects on the protein must be rather stabilizing.

A number of studies have also indicated that a relatively higher frequency of aromatic residues in thermophilic proteins (Kumar et al., 2000; Pack and Yoo, 2004). While this appears to be true for tyrosines (CHOLOX: 20, BCO: 17), there were less phenylalanines (CHOLOX: 19, BCO: 21) and tryptophanes (CHOLOX: 18, BCO: 19) observed in CHOLOX (Fig. 6). Moreover, the number of pi-interactions was increased only slightly (CHOLOX: 20, BCO: 18) (Fig. 7). The structural distribution of the non-homologous phenylalanines, tryptophanes and tyrosines (Phe: 7, Trp: 1 aa, Tyr: 13 aa), also, was almost entirely located on the protein's outer periphery (Fig. S5, Supporting Materials) and not in its core.

4. Discussion

Even though cholesterol oxidase from *B. sterolicum* and the enzyme from *Chromobacterium* sp. catalyze the same fundamental reaction efficiently, both enzymes differ dramatically in their respective catalytic yields with regards to temperature, organic solvents, and detergents. A detailed experimental survey of physical parameters has demonstrated that CHOLOX remained mostly functional at very high temperatures as well as in the presence of aggressive detergents like SDS and many other water/organic solvent mixtures (Doukyu and Aono, 1998). Most astonishingly, and in contrast to the other enzymes, the studies also showed that this enzyme still remained functional, when a combination of such physical conditions was applied. As a result, the enzyme is to be considered the most stable among all oxidases tested thus far (Doukyu, 2009; Doukyu and Aono, 2001).

At this point it is unclear as to how the structure was stabilized phylogenetically. *Chromobacterium* sp. DS-1 was isolated from soil near a lake, i.e. under non-extreme conditions. As the enzyme was derived from a mesophilic organism, it seems unlikely that evolutionary pressures on the organism have resulted in an enzyme through a selection for high-temperature resistancy. In order to

make the substrate cholesterol accessible to the organism in the screening procedure, the bacteria were successfully cultivated on agar medium containing relatively high concentrations of detergents (0.34% Triton X-100 and 64 mM sodium cholate) (Doukyu, 2009; Doukyu et al., 2008). Nonetheless, it remains to be shown if this organism has actually evolved to survive in extreme environmental conditions and whether other of its proteins also exhibit such outstanding physical properties.

Generally, thermophilic proteins often exhibit statistically preferred physical properties that maintain structure and catalytic activity at high temperatures in contrast to their mesophilic counterparts. While the comparisons of sequences and structures have not revealed any single-most important cause for increased thermal stability, it is commonly accepted that subtle enhancements of stabilizing interactions throughout the entire molecules are likely to have an overall synergistic effect. By and large, systematic comparisons of homologous proteins from both classes have revealed that thermal stability can be achieved through higher core hydrophobicity, increased packing density, smaller surface loop structures as well as through maximization of interactions such a ionic- and hydrogen bonds and covalent interactions (Kumar and Nussinov, 2001; Paiardini et al., 2008; Perl and Schmid, 2002).

The outstanding stability of CHOLOX vs. BCO thus appears to exemplify an unusual conundrum: despite its dramatically increased stability, the protein exhibits a suspicious lack of residue properties that are typically associated with thermophilic or thermostable proteins. As can be seen in Figs. 6 and 7, CHOLOX carried less charged residues, less main-chain/side-chain and side-chain/side-chain interactions (as defined and determined by PIC (Tina et al., 2007)). Moreover, CHOLOX also exhibited a substantially larger overall cavity volume than its less stable counterpart.

Structural comparisons of homologous proteins, in general, show that the hydrophobic core is the most conserved structure. Statistical and experimental studies suggest that the packing of buried apolar residues contribute substantially to the stability of a protein (Criswell et al., 2003; Vogt and Argos, 1997). The structural comparisons of CHOLOX to BCO, however, do not provide a simple backing for this idea either. Rather, the almost indistinguishable packing densities and buried surface areas of the two proteins, and the increased cavity volume of CHOLOX seem to contradict these findings (compare Table 2).

In this study, we have focused our attention on the location of non-conserved (“new”) residues in order to elucidate the factors that contribute to its superior stability. Generally, only two types substitutions were observed: (1) substitutions that are distributed throughout the protein and (2) substitutions that are almost exclusively found on or near the surface of the protein. Remarkably, out of the 20 amino acids that were mapped onto the structure only the “new” isoleucines, threonines and to some degree valines were found to be distributed throughout the core of the protein. Statistically however, none of these residues are known to significantly enhance protein stability in thermophilic proteins. Furthermore, as these residues mostly replaced alanines, glycines, methionines, serines, leucines, threonines and valines, these substitutions have not resulted in any significantly improved repacking of the core either as judged by Voronoi packing density calculations and the amount of buried hydrophobic surface area (Table 2).

Calculations of the hydrophobic surface area with the program CHASA (Fleming and Richards, 2000; Fleming et al., 2005), also, revealed no significant differences between the two structures. Whereas CHOLOX exhibits 7796.7 $Å^2$ of hydrophobic surface area with the corresponding solvation energy of −389 kal/mol, BCO shows a marginally larger surface area of 8083.02 $Å^2$ (solvation energy: −374 kcal/mol). We therefore do not believe that differences in buried hydrophobic surface area majorly contribute to CHOLOX’s dramatically increased stability. The core substitutions, however, have led to a reduction of buried polar surface area (Table 2), which may have contributed to a net stabilization. Such optimizations of a protein’s core were also observed in a statistical survey between mesophilic and thermophilic proteins (Spassov et al., 1995).

What is remarkable in this case is that the vast majority of substitutions that are known to significantly contribute to stability (i.e. charged, polar, large hydrophobic residues) were found almost exclusively on or near the solvent exposed surface. This even holds true for all the large aromatic residues including leucine, phenylalanine, tyrosine and tryptophane. Not surprisingly, the overall majority of charged or polar residues, as well as other substantially populated residues such as glycine, proline, asparagine and glutamine (Figs. S5 and S6 (Supporting Information)) were also found on the protein’s surface. In particular the distribution of charges appeared substantially different in both proteins as can be seen in Fig. 5. It may thus be reasonable to speculate that a favorable reduction of repulsive interactions rather than an increase of salt bridges contribute to the enhanced stability of CHOLOX (Spassov and Atanasov, 1994).

At this point it should also be noted that an improvement of the quality of interactions may be of greater importance than a larger quantity. For example, theoretical studies of ionic interactions of mesophilic and hypothermophilic proteins suggests that an optimal positioning of salt bridges can contribute greatly to thermal stability rather than an increase of the their numbers (Danciulescu et al., 2007). This study is of interest as it takes into account the dynamic behaviors of the protein, its corresponding side chains and the solvent at elevated as well as at mesophilic temperatures. Further work, however, is required to confirm these concepts.

The observation of a hyperthermostable enzyme from a mesophilic organism, may thus point to new ways to engineer thermally stable proteins *via* rational protein design and combinatorial methods. Previous successful attempts to generate organic solvent stable enzymes *via* directed evolution have been reported (Spiller et al., 1999). Most of the few resulting mutations, however, appeared to have stabilized surface exposed loop structures rather than other areas in the core of the protein. The extensive substitutions of residues near the solvent exposed surface structures of CHOLOX are also likely to stabilize surface structures as well. Both of these observations may therefore point to a new way to test the importance of selective surface modifications to dramatically increase stability. Using combinatorial methodologies, targeted substitutions of these peripheral areas could be explored specifically to select and identify proteins with improved organic solvent or thermal stabilities. In particular, the systematic application of organic solvents rather than temperature in the selection procedures could possibly be used to evolve enzymes with unprecedented physical properties and stabilities.

In conclusion, we suggest that the use of statistically derived amino acid contents and properties of thermophilic proteins can be misleading in the identification of thermally stable proteins. Even though CHOLOX’s stability rivals that of many hyperthermophilic proteins, it does not exhibit the typically observed structural properties or residue statistics. Although the substitutions observed in CHOLOX were consistent with previous findings in that the core of a protein tends to be the most conserved structure, most of its significant changes occur on or near the solvent exposed surface.

Although it is not possible to understand the importance of each substitution to the protein’s stability solely based on this structure, we propose that the protein’s stabilization against solvents and temperature may, in part, be stabilized through a specific stabilizations of secondary structures on its surface. Engineering a protein with a combination of enhanced thermal- and solvent-stability may therefore also be accomplished through selective surface engineering rather than by redesigning an entire protein core.

Acknowledgments

The authors are grateful for the expert help received from Drs. P. Dunten, I. Mathews and T. Doukov at Beamlines 7-1 and 9-1 of the Stanford Synchrotron Research Laboratory. The authors are indebted to Pat Fleming for help with CHASA calculations. This work was in part supported by the International Training Program (ITP) from the Japanese Society for the Promotion of Science (JSPS).

Appendix A. Supplementary data

Supplementary data associated with this article can be found, in the online version, at doi:10.1016/j.jsb.2010.01.012.

References

Adams, P.D., Pannu, N.S., Read, R.J., Brunger, A.T., 1997. Cross-validated maximum likelihood enhances crystallographic simulated annealing refinement. Proc. Natl. Acad. Sci. USA 94, 5018–5023.

Arnott, M.A., Michael, R.A., Thompson, C.R., Hough, D.W., Danson, M.J., 2000. Thermostability and thermoactivity of citrate synthases from the thermophilic and hyperthermophilic archaea, *Thermoplasma acidophilum* and *Pyrococcus furiosus*. J. Mol. Biol. 304, 657–668.

Arya, S.K., Solanki, P.R., Datta, M., Malhotra, B.D., 2009. Recent advances in self-assembled monolayers based biomolecular electronic devices. Biosens. Bioelectron. 24, 2810–2817.

Baker, N.A., Sept, D., Joseph, S., Holst, M.J., McCammon, J.A., 2001. Electrostatics of nanosystems: application to microtubules and the ribosome. Proc. Natl. Acad. Sci. USA 98, 10037–10041.

Blaber, M., Zhang, X.J., Matthews, B.W., 1993. Structural basis of amino acid alpha helix propensity. Science 260, 1637–1640.

Blaber, M., Baase, W.A., Gassner, N., Matthews, B.W., 1995. Alanine scanning mutagenesis of the alpha-helix 115–123 of phage T4 lysozyme: effects on structure, stability and the binding of solvent. J. Mol. Biol. 246, 317–330.

Blaber, M., Zhang, X.J., Lindstrom, J.D., Pepiot, S.D., Baase, W.A., Matthews, B.W., 1994. Determination of alpha-helix propensity within the context of a folded protein. Sites 44 and 131 in bacteriophage T4 lysozyme. J. Mol. Biol. 235, 600–624.

Brunger, A.T., Adams, P.D., Clore, G.M., DeLano, W.L., Gros, P., Grosse-Kunstleve, R.W., Jiang, J.S., Kuszewski, J., Nilges, M., Pannu, N.S., Read, R.J., Rice, L.M., Simonson, T., Warren, G.L., 1998. Crystallography & NMR system: a new software suite for macromolecular structure determination. Acta Crystallogr. D Biol. Crystallogr. 54, 905–921.

CCP4, 1994. The CCP4 suite: programs for protein crystallography. Acta Crystallogr. D Biol. Crystallogr. 50, 760–763.

Chakravarty, S., Varadarajan, R., 2000. Elucidation of determinants of protein stability through genome sequence analysis. FEBS Lett. 470, 65–69.

Coulombe, R., Yue, K.Q., Ghisla, S., Vrielink, A., 2001. Oxygen access to the active site of cholesterol oxidase through a narrow channel is gated by an Arg-Glu pair. J. Biol. Chem. 276, 30435–30441.

Criswell, A.R., Bae, E., Stec, B., Konisky, J., Phillips Jr., G.N., 2003. Structures of thermophilic and mesophilic adenylate kinases from the genus *Methanococcus*. J. Mol. Biol. 330, 1087–1099.

Danciulescu, C., Ladenstein, R., Nilsson, L., 2007. Dynamic arrangement of ion pairs and individual contributions to the thermal stability of the cofactor-binding domain of glutamate dehydrogenase from *Thermotoga maritima*. Biochemistry 46, 8537–8549.

Doukyu, N., 2009. Characteristics and biotechnological applications of microbial cholesterol oxidases. Appl. Microbiol. Biotechnol. 83, 825–837.

Doukyu, N., Aono, R., 1998. Purification of extracellular cholesterol oxidase with high activity in the presence of organic solvents from *Pseudomonas* sp. strain ST-200. Appl. Environ. Microbiol. 64, 1929–1932.

Doukyu, N., Aono, R., 2001. Cloning, sequence analysis and expression of a gene encoding an organic solvent- and detergent-tolerant cholesterol oxidase of *Burkholderia cepacia* strain ST-200. Appl. Microbiol. Biotechnol. 57, 146–152.

Doukyu, N., Shibata, K., Ogino, H., Sagermann, M., 2008. Purification and characterization of *Chromobacterium* sp. DS-1 cholesterol oxidase with thermal, organic solvent, and detergent tolerance. Appl. Microbiol. Biotechnol. 80, 59–70.

Doukyu, N., Shibata, K., Ogino, H., Sagermann, M., 2009. Cloning, sequence analysis, and expression of a gene encoding *Chromobacterium* sp. DS-1 cholesterol oxidase. Appl. Microbiol. Biotechnol. 82, 479–490.

Egorova, K., Antranikian, G., 2005. Industrial relevance of thermophilic archaea. Curr. Opin. Microbiol. 8, 649–655.

Fleming, P.J., Richards, F.M., 2000. Protein packing: dependence on protein size, secondary structure and amino acid composition. J. Mol. Biol. 299, 487–498.

Fleming, P.J., Fitzkee, N.C., Mezei, M., Srinivasan, R., Rose, G.D., 2005. A novel method reveals that solvent water favors polyproline II over beta-strand conformation in peptides and unfolded proteins: conditional hydrophobic accessible surface area (CHASA). Protein Sci. 14, 111–118.

He, M.M., Wood, Z.A., Baase, W.A., Xiao, H., Matthews, B.W., 2004. Alanine-scanning mutagenesis of the beta-sheet region of phage T4 lysozyme suggests that tertiary context has a dominant effect on beta-sheet formation. Protein Sci. 13, 2716–2724.

Heinz, D.W., Baase, W.A., Matthews, B.W., 1992. Folding and function of a T4 lysozyme containing 10 consecutive alanines illustrate the redundancy of information in an amino acid sequence. Proc. Natl. Acad. Sci. USA 89, 3751–3755.

Holm, L., Kääriäinen, S., Rosenström, P., Schenkel, A., 2008. Searching protein structure databases with DaliLite v.3. Bioinformatics 24 (23), 2780–2781.

Humphrey, W., Dalke, A., Schulten, K., 1996. VMD: visual molecular dynamics. J. Mol. Graph. 14 (33–38), 27–28.

Kabsch, W., 1993. Automatic processing of diffraction data from crystals of initially unknown symmetry and cell constants. J. Appl. Crystallogr. 26, 795–800.

Karshikoff, A., Ladenstein, R., 1998. Proteins from thermophilic and mesophilic organisms essentially do not differ in packing. Protein Eng. 11, 867–872.

Kleywegt, G.J., Jones, T.A., 1994. Detection, delineation, measurement and display of cavities in macromolecular structures. Acta Crystallogr. D Biol. Crystallogr. 50, 178–185.

Kumar, S., Nussinov, R., 2000. Fluctuations between stabilizing and destabilizing electrostatic contributions of ion pairs in conformers of the c-Myc-Max leucine zipper. Proteins 41, 485–497.

Kumar, S., Nussinov, R., 2001. How do thermophilic proteins deal with heat? Cell. Mol. Life Sci. 58, 1216–1233.

Kumar, S., Tsai, C.J., Nussinov, R., 2000. Factors enhancing protein thermostability. Protein Eng. 13, 179–191.

Lin, L., Pinker, R.J., Phillips, G.N., Kallenbach, N.R., 1994. Stabilization of myoglobin by multiple alanine substitutions in helical positions. Protein Sci. 3, 1430–1435.

MacLachlan, J., Wotherspoon, A.T., Ansell, R.O., Brooks, C.J., 2000. Cholesterol oxidase: sources, physical properties and analytical applications. J. Steroid Biochem. Mol. Biol. 72, 169–195.

Murshudov, G.N., Vagin, A.A., Dodson, E.J., 1997. Refinement of macromolecular structures by the maximum-likelihood method. Acta Crystallogr. D Biol. Crystallogr. 53, 240–255.

Pack, S.P., Yoo, Y.J., 2004. Protein thermostability: structure-based difference of amino acid between thermophilic and mesophilic proteins. J. Biotechnol. 111, 269–277.

Paiardini, A., Sali, R., Bossa, F., Pascarella, S., 2008. "Hot cores" in proteins: comparative analysis of the apolar contact area in structures from hyper/thermophilic and mesophilic organisms. BMC Struct. Biol. 8, 14.

Pattabiraman, N., Ward, K.B., Fleming, P.J., 1995. Occluded molecular surface: analysis of protein packing. J. Mol. Recognit. 8, 334–344.

Perl, D., Schmid, F.X., 2002. Some like it hot: the molecular determinants of protein thermostability. ChemBioChem 3, 39–44.

Piubelli, L., Pedotti, M., Molla, G., Feindler-Boeckh, S., Ghisla, S., Pilone, M.S., Pollegioni, L., 2008. On the oxygen reactivity of flavoprotein oxidases: an oxygen access tunnel and gate in *Brevibacterium sterolicum* cholesterol oxidase. J. Biol. Chem. 283, 24738–24747.

Spassov, V.Z., Atanasov, B.P., 1994. Spatial optimization of electrostatic interactions between the ionized groups in globular proteins. Proteins 19, 222–229.

Spassov, V.Z., Karshikoff, A.D., Ladenstein, R., 1995. The optimization of protein-solvent interactions: thermostability and the role of hydrophobic and electrostatic interactions. Protein Sci. 4, 1516–1527.

Spiller, B., Gershenson, A., Arnold, F.H., Stevens, R.C., 1999. A structural view of evolutionary divergence. Proc. Natl. Acad. Sci. USA 96, 12305–12310.

Sundaralingam, M., Sekharudu, Y.C., 1989. Water-inserted alpha-helical segments implicate reverse turns as folding intermediates. Science 244, 1333–1337.

Tina, K.G., Bhadra, R., Srinivasan, N., 2007. PIC: protein interactions calculator. Nucleic Acids Res. 35, W473–W476.

Trapani, S., Navaza, J., 2008. AMoRe: classical and modern. Acta Crystallogr. D Biol. Crystallogr. 64, 11–16.

Vogt, G., Argos, P., 1997. Protein thermal stability: hydrogen bonds or internal packing? Fold Des. 2, S40–S46.

Voss, N.R., Gerstein, M., 2005. Calculation of standard atomic volumes for RNA and comparison with proteins: RNA is packed more tightly. J. Mol. Biol. 346, 477–492.

Wu, X.J., Choi, M.M., 2003. Hydrogel network entrapping cholesterol oxidase and octadecylsilica for optical biosensing in hydrophobic organic or aqueous micelle solvents. Anal. Chem. 75, 4019–4027.

Zhang, X.J., Baase, W.A., Matthews, B.W., 1991. Toward a simplification of the protein folding problem: a stabilizing polyalanine alpha-helix engineered in T4 lysozyme. Biochemistry 30, 2012–2017.